

PREDICTION OF BURST PRESSURE ON STEEL PIPES USING
GURSON-TVERGAARD-NEEDLEMAN (GTN) MODEL

CHONG KIM SUNG

Report submitted in partial fulfillment of the requirements for the award of the degree of
Bachelor of Mechanical Engineering

Faculty of Mechanical Engineering
UNIVERSITI MALAYSIA PAHANG

JUNE 2013

ABSTRACT

A micromechanical model of ductile fracture is applied for API X65 steel to predict ductile failure of a full-scale API X65 pipes with simulated corrosion and defects under internal pressure. The micromechanical model is the Gurson model, incorporating void nucleation, growth and coalescence where the burst pressure is predicted based on the critical void volume fraction. The present study involves experimental comparison and numerical studies of the burst pressure of pipe under ductile fracture. The main objective of the present study is to determine the burst pressure of steel pipe using GursonTevaagard model. For the experimental, the results are from the previous research journal. For the finite element analysis, the pipe model is modeled as a 3 dimensional, quarter-model in MSC.PATRAN with MSC.MARC as nonlinear implicit solver. Results with proposed ductile fracture model indicates that predicted failure pressure attain maximum load for all cases, and are in good agreement with experimental data. It also showed that the burst pressure is decreasing for increasing defect depth and length. For the characters of void volume fraction, f , it can be seen that once the void reach void growth, it soon come to void coalescence, where the burst pressures are predicted at critical void and then fracture. The results from gouge defect varies in length is analyze based on the equivalent plastic strain, ε_p and the stress

triaxially, $T = \frac{\sigma_m}{\sigma_e}$ where void growth dependent on this two key quantities. Void

volume fraction are examined based on the equivalent plastic strain and stress triaxiality on the normalize distance along the defect length and depth. It is found that distribution of equivalent plastic strain agreed well with the void volume fraction and the critical point occur at the defect tip along the defect depth and length.

ABSTRAK

Satu model micromechanical patah mulur dipohon API X65 keluli untuk meramalkan kegagalan mulur daripada skala penuh API X65 paip dengan kakisan simulasi dan kecacatan di bawah tekanan dalaman. Model micromechanical adalah model Gurson, menggabungkan sah penukleusan, pertumbuhan dan tautan di mana tekanan pecah diramalkan berdasarkan kekosongan kritikal jumlah kecil. Kajian ini melibatkan perbandingan eksperimen dan kajian berangka tekanan pecah paip bawah patahmulur. Objektif utama kajian ini adalah untuk menentukan tekanan pecahpaip keluli menggunakan Gurson model Tevaagard. Bagi eksperimen, keputusan adalah dari jurnal penyelidikan sebelumnya. Untuk analisis unsur terhingga, model paip dimodelkan sebagai satu dimensi, suku model 3 dalam MSC.PATRAN dengan MSC.MARC sebagai penyelesaian tersirat linear. Keputusan dengan cadangan model patahmulur menunjukkan bahawa tekanan kegagalan meramalkan mencapai beban maksimum bagi semua kes, dan berada dalam perjanjian yang baik dengan data eksperimen. Ia juga menunjukkan bahawa tekanan pecah semakin berkurangan untuk meningkatkan kedalaman kecacatan dan panjang. Untuk watak-watak tidak sah jumlah pecahan, f , ia boleh dilihat bahawa apabila tidak sah mencapai pertumbuhan tidak sah, ia tidak lama lagi dating untuk membatalkan tautan, di mana tekanan pecah diramalkan di sah kritikal dan kemudian patah. Hasil daripada menipu kecacatan berbeza panjang adalah menganalisis berdasarkan tekanan bersamaan plastik, ε_p dan tekanan triaxially,

$T = \frac{\sigma_m}{\sigma_e}$ di mana pertumbuhan tidak sah ini bergantung kepada dua kuantiti utama.

Tidak sah jumlah kecil diperiksa berdasarkan tekanan bersamaan plastic dan triaxiality tekanan pada jarak normal sepanjang kecacatan dan mendalam. Ia didapati bahawa taburan terikan plastic bersamaan juga bersetuju dengan jumlah kecil tidaksah dan titik kritikal berlaku pada hujung kecacatan sepanjang kedalaman kecacatan dan panjang.

TABLE OF CONTENTS

	Page
EXAMINERS' APPROVAL DOCUMENT	ii
SUPERVISOR'S DECLARATION	iii
STUDENT'S DECLARATION	iv
DEDICATION	v
ACKNOWLEDGEMENTS	vi
ABSTRACT	vii
ABSTRAK	viii
TABLE OF CONTENTS	ix
LIST OF TABLES	xiii
LIST OF FIGURES	xiv
LIST OF SYMBOLS	xvii
LIST OF ABBREVIATIONS	xix
 CHAPTER 1 INTRODUCTION	
 1.1 Background of Study	1
1.2 Problem statement	3
1.3 Objectives	3
1.4 Scopes	3
1.5 Significance of project	4
 CHAPTER 2 LITERATURE REVIEW	
 2.1 Introduction	5
2.2 Burst Pressure	8
2.2.1 Von Mises yield criteria	8
2.2.2 Steel pipe	10
 2.3 Major Corrosions in Pipelines carrying Gas and Crude Oil	10
2.3.1 Factors that contribute to external corrosion in pipelines	12
2.3.2 Factor that contribute to internal corrosion in pipelines	13

2.3.3	Corrosion Mechanism on pipeline	14
2.3.3.1	Electrochemical corrosion	14
2.3.3.2	Chemical corrosion	15
2.3.3.3	Mechanical corrosion	16
2.4	Types of Cracks	17
2.5	Strain Based Failure Criterion (Micromechanical model)	18
2.5.1	Ductile Fracture	19
2.5.1.1	Void Nucleation	21
2.5.1.2	Void Growth	21
2.6	Classification of Micromechanical model	24
2.6.1	Coupled Micromechanical modelling	24
2.6.2	Evolution of GTN model	27
2.6.3	Uncoupled Micromechanical modelling	29
2.6.3.1	Void Growth Model (VGM)	29
2.6.3.2	Stress Modified Critical Strain Model (SMCS)	30
2.6.4	Criteria in developing ductile fracture prediction	31
2.6.5	Determination of Gurson parameters	33
2.6.5.1	Determination of f_0 and f_F computational cells	34
2.6.5.2	Determination of Gurson model parameters	35
2.7	Comparison between the Three Proposed Models	38
2.8	Experimental Investigation	40
2.8.1	Tensile Test	41
2.8.1.1	Stress-strain Diagram	41
2.8.2	Burst Test	42
2.8.2.1	Full scale Burst tests of Corrosion Defects	43
2.9	Stress Based Failure Criterion (Closed formed Method)	44
2.9.1	ASME B31G	45
2.9.2	Modified B31G Criterion	47
2.9.3	DNV RP-F-101 Criterion	48
2.9.4	PCORRC Criterion	49
2.10	Comparison among experimental method and micromechanical method	51

CHAPTER 3 METHODOLOGY

3.1	Introduction	53
3.2	Determination of experimental data and material	55
	3.2.1 Determination of material properties	55
	3.2.2 Determination of experimental data	57
3.3	Finite element analysis	59
	3.3.1 FE modeling	60
	3.3.2 Load case, Boundary conditions and loads	61
3.4	Validation using Closed form calculations and SMCS	62
	3.4.1 Closed form calculations	62
	3.4.2 SMCS	63

CHAPTER 4 RESULTS AND ANALYSIS

4.1	Finite element analysis results	65
4.2	Results comparison and analysis	66
	4.2.1 Application to failure predictions of corroded API X65 pipes	69
	4.2.1.1 Comparisons	69
	4.2.2 Application to failure predictions of API X65 pipes with gouges	69
	4.2.2.1 Comparisons	69
4.3	Discussions	80
	4.3.1 Summary of comparisons	80
	4.3.2 Limitations of Present Study	81

CHAPTER 5 CONCLUSION

5.1	Conclusion	82
5.2	Recommendations	83
	REFERENCES	84

APPENDICES

A1	True Stress-Strain data at room temperature for API X65 Steel	88
A2	Data collected and calculated for Gouge Defect, 50%, l=100mm	89
	Gantt Chart (Semester 1)	101
	Gantt Chart (Semester 2)	102

LIST OF TABLES

Table No.	Title	Page
2.1	Mechanical properties of various grades of pipelines steel	10
2.2	GTN model parameter values for API X65 steel	35
2.3	GTN model parameter values from the literature	36
2.4	Differences and similarities between GTN, VGM and SMCS model	39
3.1	Mechanical tensile properties at room temperature of the API X65 steel, used in the present work	56
3.2	Dimensions for the pipe design.	57
3.3	Defect design dimension and experiment data for rectangular defect.	58
3.4	Dimensions and experiment data for gouge defect.	59
3.5	GTN parameters for API X65 steel.	60
3.6	Number of elements for mesh seeds for FE model.	60
3.7	Boundary conditions applied on the pipe model.	62
4.1	Value of σ_{max} reached for different depths, d.	66
4.2	Burst pressure predicted for FEA and design codes for different depths	66
4.3	Comparison between burst pressure for experimental FE and	67
4.4	Burst pressure comparison for gouge defect of 50%.	70
4.5	Burst pressure comparison for gouge defect of 75%.	70

LIST OF FIGURES

Figure No.	Title	Page
2.1	Method of experimental, strain based model and strain based model used in predicting burst pressure of steel pipe in present study	7
2.2	Reducing in thickness of pipe thickness due to wall thinning	12
2.3	Pipeline corrosion in different soils	13
2.4	Pitting Corrosion	15
2.5	Classification of crack in pipeline	17
2.6	Axial planar flaw and non-planar flaws (axially and circumferentially long) in a pipe	18
2.7	Longitudinal cracks circumferential cracking	18
2.8	Ductile fracture process	20
2.9	Sequence of damage mechanisms	22
2.10	Ductile fracture mechanism on void following authors	23
2.11	The authors and extending that involved in modifying Gurson model.	28
2.12	Modeling of ductile crack growth using computational cells	34
2.13	Specimen after tensile test and the graph of force with elongation of the specimen	40
2.15	Full engineering stress strain curve	42
2.17	Methods for corrosion assessment including codified and other methods	44
2.18	Longitudinal extent of the corrosion area	46
2.19	Assumed parabolic corroded area for relatively short corrosion defect	50
2.20	Assumed rectangular corroded area for longer corrosion defect	46
2.21	Assumed $A_c = 0.85dL$ method for corrosion defect	47
2.22	Comparison among experimental method, strain based and stress based micromechanical method	51
3.1	Overall Flowchart Research	54
3.2	Procedure in Patran Analysis	55

3.3	Tensile specimen	56
3.4	True stress-strain data for AP1 5L X65 steel at room temperature	56
3.5	Pipe with simulated corrosion defect	57
3.6	Pipe with gouge defect design	57
3.7	2 Dimensional of the pipe	59
3.8	FE model for a quarter of pipe model using MSC.PATRAN	60
3.9	Boundary conditions applied on the pipe model	62
4.1	Void volume fraction contour profile for the pipe	64
4.2	A typical finite element mesh for pipe with gouges and the contour markers showing void volume fraction profile at the final time step 1s. The critical void happens at the tip of the defect	65
4.3	Comparison between the void volume fractions for different defect depth on the pressure increment	65
4.4	Comparison on the burst pressure for different defect depth for FEA, experimental and Equation 4.1	68
4.5	Relationship between burst pressure and defect depth for different design codes and FEA.	69
4.6	Comparison of burst pressure for the case of defect length 50%.	71
4.7	Comparison for Equation 4.2 and Equation 4.3 for gouge defect of different length.	74
4.8	Distributions of stress triaxiality and equivalent strain for pipes with gouge along the defect length: (a) MNA pipe test and (b) MNB pipe test and (c) MNC pipe test and (d) MND pipe test and (e) MNE pipe test	74
4.9	Distribution of void volume fraction over the normalized distance on the defect depth following the variation of defect length, MNA(100mm), MNB(200mm), MNC(300mm), MND(400mm), and MNE(600mm) with case 50% depth	75
4.10	Distribution of strain equivalent over the normalized distance on the defect depth following the variation of defect length, MNA(100mm), MNB(200mm), MNC(300mm), MND(400mm), and MNE(600mm) with case 50% depth.	76
4.11	Distributions of stress triaxiality and equivalent strain for pipes with	77

	gouges along the defect depth from the inner surface to the notch tip of the defect	
4.12	Distribution of Void volume fraction over the defect depth with varied with the defect length, MNC (300mm), MND (400mm) and MND (600mm) for the case 50% depth	78
4.13	Distribution of strain equivalent over the defect depth with varied with the defect length, MNC (300mm), MND (400mm) and MND (600mm) for the case 50% depth	79

LIST OF SYMBOLS

P_y	Internal pressure on the onset of yield
P_u	Ultimate pressure
$\sigma_{Vonmises}$	Von Mises yield criteria
σ_1	Ratio of the applied tensile force F to the metal area A
ε_i	Strain at onset of instability
n	Strain coefficient
D	Pipe outer diameter
t	Pipe wall thickness
k	Strength coefficient
c	Defect width
L	Pipe length
l	Defect length
d	Defect depth
P_{exp}	Experimental pressure
V_{Void}	Volume of voids
V_{Matrix}	Volume of matrix
f	Void volume fraction
σ_y	Yield stress
ϕ	Non-dilatational strain energy
σ_0	Von Mises effective stress

q_1	Tvergaard coefficients describing the plastic properties of the material
f^*	Actual void volume fraction
σ_m	Hydrostatic pressure (mean stress)
σ_{eq}	Von Mises effective stress
f_c	Critical void volume fraction
f_F	Void volume fraction corresponding to the loss of material strength
ε_{ii}^{*P}	Plastic part of the strain rate tensor
$(R/R_0)_c$	Critical void growth ratio
$d\varepsilon_{eq}^P$	Equivalent plastic strain increment
α	Material constant
ε_f	Fracture strain
T	Stress triaxiality
ε_{eq}	Strain equivalent

LIST OF ABBREVIATIONS

FE	Finite Element
SMCS	Stress modified fracture criteria
ASME	American Society for Mechanical Engineer
Eq.	Equation
UTS	Ultimate Tensile Strength
GTN	GursonTevargaard model
VGM	Void Growth model
API	American Petroleum Institute

Chapter 1

INTRODUCTION

1.1 BACKGROUND OF STUDY

Pipelines are one of the major means of transporting hydrocarbons (oil and natural gas) from one point to the other point, which may be routed within onshore or offshore locations. There is a great risk that defects will occur during the service life of these pipelines. Corrosion, either internal or external is one of the common defects observed in many instances. With the passage of time the corrosion that occurs either at a localized point or onto a large area cause the metal loss and hence the strength or in other words load bearing capacity of the pipeline is reduced. Corrosion induced micromechanical ductile fracture in pipe body due to the growth of void and coalescence in the materials which will lead to plastic deformation that cause bursting of pipe. The prediction of burst pressure is based on the ultimate pressure, $P_u > P_y$ yield pressure (Antaki, G.A., 2003). Also, identification of different types of corrosion can help in applying the suitable analysis method and solution. Hence, predictive measurement on defect assessment for high pressure piping is important aimed at quantifying the impacts of the defects and for safety precautions procedure.

An initiative has been taken by the European gas transmission system operators on the frequencies and probabilities study that cause incidents in pipelines. (8th Report of EGIG, Dec 2011). It is divided into two groups, first, the primary failure frequency which is by the external interference, corrosion material defect, ground movement and others. The other is secondary failure frequencies which consider the influence of design parameters (pressure, diameter, wall thickness, etc.) The external interference the activity having caused the incident such as digging, piling, and equipment involved in incident. Next, corrosion includes the location either internal or external, and the

corrosion type. Then the material failure, which is the type of defect, next is ground movement like erosion, flood and others. The installation of the annual length of pipelines was equal to 129,719 km in 2007 and increase to 135,211 km in 2010. Also, the incidents were reported of total 1,249 cases over the period 1970-2010 with primary failure frequency per 1000km-yr is 0.372. Whereas for an interval of 5 years between 2006-2010, the number of incidents occurs are 106 cases and the primary failure frequency per 1000km-yr is 0.162. In fact, external interference is highest incidents causes with contribution Of 48.4% followed by material failure and corrosion with 16.7% and 16.1% respectively. From the statistics, except for the external interference incident causes, from the view of internal, that is the material failure and corrosion, it have given a big impact on the incident occur in pipelines. Hence, a careful study and analysis need to be carried out to ensure the integrity of pipeline service in this oil and gas field.

In fact, numerous experiments on the material failure and corrosion which is the impact of defects and analytical researches has been done especially on the burst pressure predictions of pipelines but this entire are still not enough to ensure its integrity. This is due to the lack of experimental and analytical researches ability in performing tests reflecting complex geometries and loading condition. As it is known that pipeline which lying on the seabed and is subjected to the physical environmental aspects must be taken care of in order to ensure its integrity. The loading conditions are referring to the physical environmental aspect which includes the oceans depth and distances, hydrostatic pressure, temperature, seawater and sea-air interface chemistry, and crude oil composition. Hence, in order to study the incidents consequence of the material failure and corrosion, the application of micromechanical model using finite element method is important to study more detail of the internal failure mechanism and sensitivity analysis can help improve the study.

1.2 PROBLEM STATEMENT

Experimental and analytical study on the material failure of steel pipe is not enough to ensure its integrity due to the lack of experimental and analytical researches ability in performing tests reflecting complex geometries and variable loading condition. Hence, Gurson model which is the micromechanical model transfer better detection of the defect analysis in studying the ductile fracture of pipeline by predicting its burst pressure. This Gurson model will be based on finite element method to study the material fracture in terms of void where the variable factors that cause pipeline fracture can be analyzed.

1.3 OBJECTIVES

The aim of this research is about the study and application of micromechanical model, GTN model in predicting pipe burst pressure. Hence, the objectives of this study are:

- i. To predict the burst pressure of steel pipe using Gurson-Tvergaard-Needleman (GTN) model.
- ii. To determine the effect of depth and length of the defect towards the failure pressure of the pipe.

1.4 SCOPE OF PROJECT

- i. The material used in this project is steel with API X65.
- ii. The outer diameter of the pipe is fixed to 762 mm, thickness 17.5 mm and length 2300 mm and it is analyses with different defect depth and length.
- iii. The defect depth of 25%, 50% and 75% and defect length of 100 mm, 200mm, 300 mm, 400 mm, and 600 mm are used in the present study.
- iv. A quarter of a full pipe was modeled due to symmetry conditions.
- v. A finite element analysis using three-dimensional elastic-plastic damage analyses were performed to simulate the pipe burst tests using Marc Patran.

- vi. The failure assessment has been compared with limit load analysis (ASME B31G, modified ASME B31G, and PCORRC)

1.5 SIGNIFICANCE OF PROJECT

In the present study, different types of defects which variant in defect depth and length is carried out to test more cases and this contributed more data which expand the scope of analysis. Besides, the prediction of burst pressure will be based on the character of void volume fraction using failure criterion approach in FEA. Unlike the previous research (Chang, S.O., 2011) where, even the Gurson model is simulated for ductile damage and failure, but the prediction of burst pressure of pipe is based on the empirical-based burst pressure equation for axial cracked pipe and also using stress modified fracture strain model. The usage of void volume fraction makes the prediction simpler as it is based on the critical void volume fraction whether it exceed or not.

CHAPTER 2

LITERATURE REVIEW

2.1 INTRODUCTION

There will be two main parts discussed in this chapter. The first part is on the material and corrosion of steel pipe. The second part will be on the method of predicting failure in pipeline of this project. For the first part, it include the von Mises yield criteria of burst pressure, where $P_u \geq P_y$. It is followed by some steel pipe standard categories. Burst pressure occurs as result of wall thinning due to corrosion. In fact, there are few categories of pipe crack, for instance, longitudinal crack, circumference crack, and spiral crack.

In the second part of the prediction of failure of structures, there are the global approaches and the local approach. (Clotilde, B., et.al. 2004). The global approach was first proposed more than 50 years ago, in the framework of linear fracture mechanics, and then extended to plasticity and viscoplasticity through nonlinear fracture mechanics about 30 years ago. Although this global approach are extremely useful, frequently used and still improving, they have been proved to suffer from several limitations; where industrial need new methodologies tools to be analyzed realistically and mastered practically. This need for new methods, combined with the development of physically-based models of mechanical behavior and micromechanical treatments, has proposed by McClintock (McMlinton, 1963) in the early 80's to the so-called “local approach to fracture”. Unlike the “global” treatment, which makes the fracture resistance of a component mainly depend on a single global parameter, whatever the damage and deformation mechanisms of the specific material under study, the “local” approach emphasizes these material specificities: it combines a detailed experimental analysis of the considered materials and of their specific damage mechanisms, a realistic modeling

of these mechanisms and the implementation of these models into a numerical simulation of the response of the structural components under investigation.

Under the local approach of fracture, depending on the model employed for simulating damage, it divided into damage based on volume which is micromechanical model and damage based on surface which is phenomenological model. Micromechanical model is divided into strain based (include uncoupled and coupled) and stress based (the design codes). The uncoupled modeling are SMCS and VGM whereas the coupled modeling is GTN. The stresses based are ASME B31G, Modified ASME B31G and PCORRC. The micromechanical model is incorporating void nucleation, growth and coalescence, for instance, the Gurson–Tvergaard–Needleman model (Tvergaard, V., 1981, 1982). The damage based on surface is using a phenomenological model for ductile fracture, which is the cohesive zone model (Chen CR, 2003). All these methods will be summarizing in the Figure 2.1.

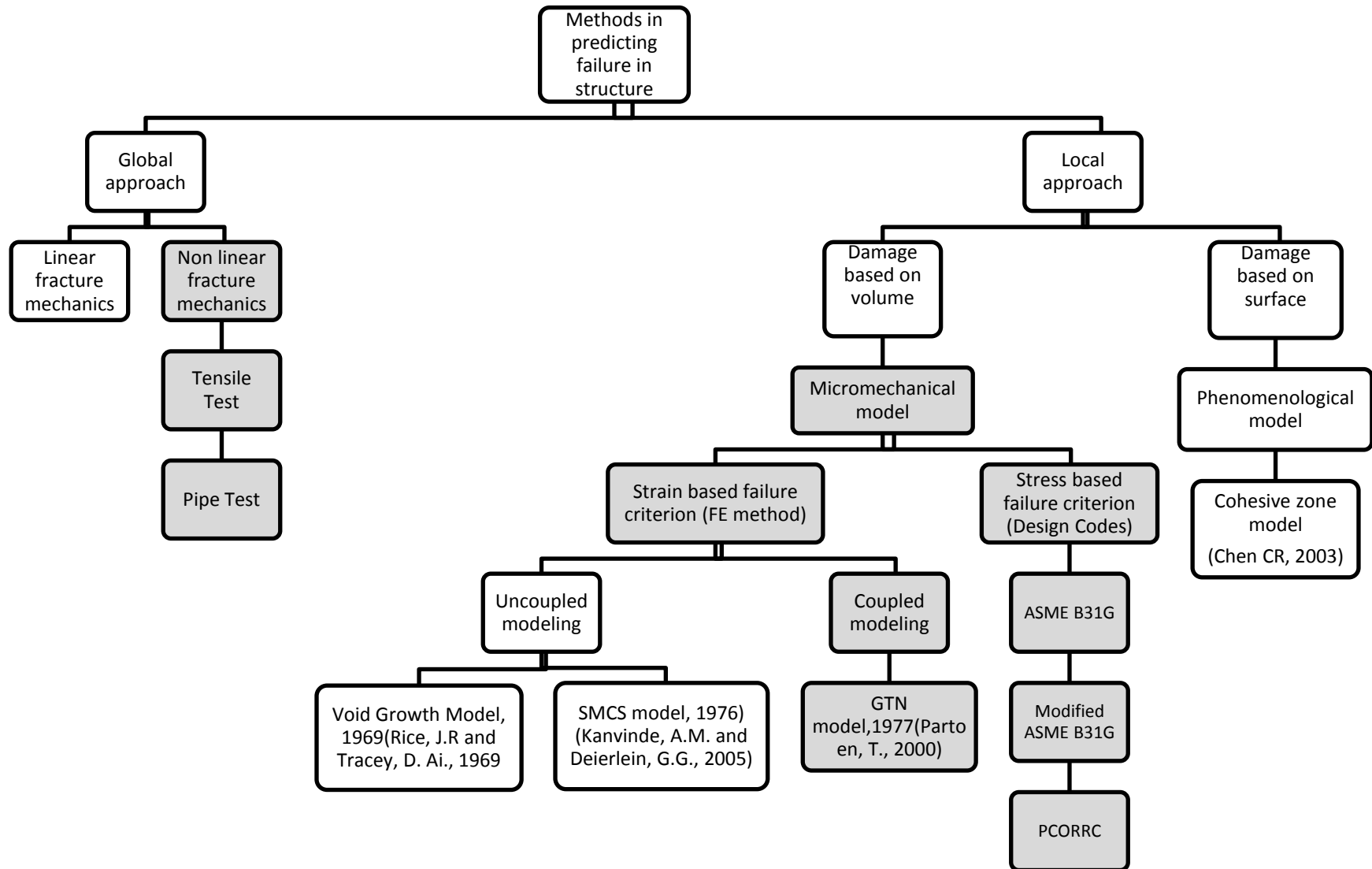


Figure 2.1: This highlight box will be the methods used in present study. The methods used in present study are the nonlinear method (pipe test), strain based method (GTN model) and stress based method (design codes) as to validate each other's.

For the present study, the methods used are those highlighted which are the non-finite element method (experimental method), finite element (FE) analysis (GTN model), and closed form method (the design codes). These three methods are important in predicting burst pressure of steel pipe as they all acts together to give verification and comparison between each other. Finite element method is important as it can greatly enhance the overall result by checking against deformation, stress or vibration specifications. Most importantly, FE analysis results identify critical areas which carry most of the load, as well as areas where material may be saved. The burst pressure from FE was then compared with values calculated using design codes for pipelines containing defects.

2.2 BURST PRESSURE

Burst pressure of steel pipe occur when corrosion induce wall thinning on the pipe and hence result in metal loss which is the failure. In fact, burst pressure occurs when $P_u \geq P_y$, where P_u is the ultimate pressure and P_y is the internal pressure at onset of yield.

2.2.1 von Mises Yield Criteria

Based on the von Mises criterion, the yielding of the pipe wall will take place when the distortion energy reaches a certain limit value $\sigma_{vonMises}$. (Antaki, G.A., 2003). This can be shown as in Eq. (2.1).

$$(\sigma_h - \sigma_1)^2 + (\sigma_1 - \sigma_r)^2 + (\sigma_r - \sigma_h)^2 = \sigma_{vonmises}^2 \quad (2.1)$$

The value $\sigma_{vonmises}$ is obtained from the tensile test. In the case, $\sigma_h = \sigma_r = 0$ and $\sigma_1 = F/A$ is the ratio of the applied tensile force F to the metal area A. In fact, yielding will take place when $\sigma_1 = S_y$, where the von Mises criterion can be written as in Eq. (2.2):

$$(0 - S_y)^2 + (S_y - 0)^2 + (0 - 0)^2 = \sigma_{vonmises}^2 = 2S_y^2 \quad (2.2)$$

By substitution, the internal pressure at which the pipe wall yields is as shown in Eq. (2.3). (Antaki, G.A., 2003).

$$P_y = \frac{S_y}{\sqrt{\frac{3}{4}\left(\frac{D}{2t}\right)^2 + \frac{3}{2}\left(\frac{D}{2t}\right) + 1}} \quad (2.3)$$

P_y =internal pressure at onset of yield, psi

For large diameter to thickness ratio ($D/t \gg 1$) we obtain the internal pressure at the onset of yield as in Eq. (2.4).

$$P_y = \frac{4tS_y}{D\sqrt{3}} \quad (2.4)$$

As the internal pressure continues to increase beyond the yield pressure, P_y , the pipe wall will bulge outward and reach a point of instability. Actually, in reality the material is not perfectly uniform and this bulging does not take place exactly uniformly around the circumference but preferentially on the side of the pipe wall. The hoop strain at which instability occurs is as shown in Eq. (2.5).

$$\varepsilon_i = n/2 \quad (2.5)$$

ε_i = strain at onset of instability

n= strain coefficient

After the instability, which is the outward bulge in pipe wall, the pipe ruptures. The pressure at ruptures is the ultimate pressure P_u given as in Eq.(2.6):

$$P_u = (2kt/D)e^{-n} \{n/[2(3/4)^{(1+n)/n}]\}^n \quad (2.6)$$

Where σ_u = ultimate pressure at burst, psi

t= pipe wall thickness, in

k= strength coefficient, psi

D=pipe outer diameter, in

2.2.2 Steel Pipe

Steel pipe is the most common pipe that has been use in global industries. This is because the material properties of the steel pipe itself. Steel is among the best material in aspect of durability and long live lasting compare to the other material. This kind of pipe normally used in many industries to transfer fluid such as oil, gas, water, chemical, smoke and others. In steel pipe itself, there are certain level or grades for differentiate the steel pipe durability. There are various grades of steel, but the common used by industries is X65, X80 and X100 steels. The higher grades mean the higher durability of the steel. Table 2.1 shows the mechanical properties for the pipelines steel.

Table 2.1: Mechanical properties of various grades of pipelines steel (Cheng, LY.2012)

Mechanical properties (steel)	X65	X80	X100	X42
Young's modulus (MPa)	207000	207000	207000	207000
Poisson's ratio	0.3	0.3	0.3	0.3
Yield Strength (MPa)	456	646	802	290
Tensile Strength (MPa)	570	760	891	420

2.3 MAJOR CORROSIONS IN PIPELINES CARRYING GAS AND CRUDE OIL

Corrosion is one of the leading that cause failure in onshore and offshore transmission pipelines. As these oil and gas pipelines play a critical role in delivering energy resources needed to power communities around the world, its causes of corrosion leading to failure are need to be identified. There are two areas of corrosion occur in pipelines: corrosion from medium carried inside the pipes (internal corrosion); also corrosion attack upon the outside of the pipes (external corrosion).